

Phase Transition and Thermal Order-by-Disorder in the Pyrochlore Quantum Antiferromagnet $\text{Er}_2\text{Ti}_2\text{O}_7$: A High-Temperature Series Expansion Study

J. Oitmaa,¹ R. R. P. Singh,² A. G. R. Day,³ B. V. Bagheri,³ and M. J. P. Gingras^{3,4,5}

¹*School of Physics, The University of New South Wales, Sydney 2052, Australia*

²*Department of Physics, University of California Davis, CA 95616, USA*

³*Department of Physics and Astronomy, University of Waterloo, Waterloo, ON, N2L 3G1, Canada*

⁴*Perimeter Institute for Theoretical Physics, 31 Caroline North, Waterloo, ON, N2L 2Y5, Canada*

⁵*Canadian Institute for Advanced Research, 180 Dundas Street West, Suite 1400, Toronto, ON, M5G 1Z8, Canada*

(Dated: May 15, 2018)

Several rare earth magnetic pyrochlore materials are well modeled by a spin-1/2 quantum Hamiltonian with anisotropic exchange parameters J_s . For the $\text{Er}_2\text{Ti}_2\text{O}_7$ material, the J_s were recently determined from high-field inelastic neutron scattering measurements. Here, we perform high-temperature (T) series expansions to compute the thermodynamic properties of this material using these J_s . Comparison with experimental data show that the model describes the material very well including the finite temperature phase transition to an ordered phase at $T_c \approx 1.2$ K. We show that high temperature expansions give identical results for different $\mathbf{q} = 0$ xy order parameter susceptibilities up to 8th order in $\beta \equiv 1/T$ (presumably to all orders in β). Conversely, a non-linear susceptibility related to the 6th power of the order parameter reveals a thermal order-by-disorder selection of the *same* non-collinear “ ψ_2 state” as found in $\text{Er}_2\text{Ti}_2\text{O}_7$.

Order-by-disorder (ObD) is a beautiful concept of central importance in the field of frustrated magnetism. [1, 2] Saddled with large accidental degeneracies, a subset of states, those that support the *largest* quantum and/or thermal fluctuations, may be selected to form true long-range order, thus turning on its head the conventional wisdom of “less fluctuations lead to more order”. While ObD has been discussed theoretically for over thirty years, and proposed to be at play in a number of experimental settings, most recently in cold atom systems, [3] convincing demonstrations of ObD in real materials have remained scarce. [4, 5] The main reason for the paucity of confirmed ObD material exemplars is that the classical degeneracies are typically not sufficiently symmetry-protected to rule out that some weak energetic perturbations are responsible for stabilizing the observed long-range order. An exception is the long-range order found in the XY pyrochlore antiferromagnet $\text{Er}_2\text{Ti}_2\text{O}_7$. [6–8] Two groups [5, 9] have recently put forward a strong case for a robust *highly protected* classical degeneracy in that system, hence making the case for ObD much more compelling than in any previous examples.

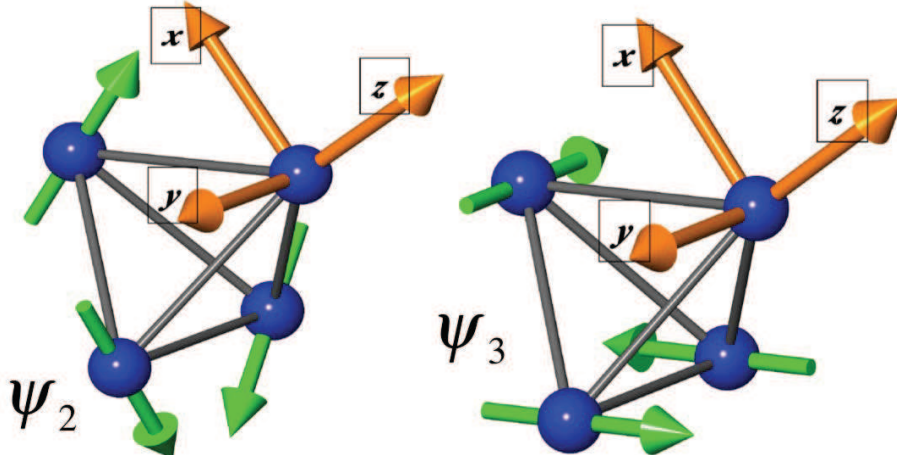


FIG. 1: The pyrochlore lattice can be described as a face-centered cubic lattice of elementary tetrahedra units. In ψ_2 (left) and ψ_3 (right), each elementary tetrahedron has the shown spin configuration with moments along the local x and y axis for ψ_2 and ψ_3 , respectively.

In an XY pyrochlore such as $\text{Er}_2\text{Ti}_2\text{O}_7$, the ordered moments lie on average in an xy plane perpendicular to their local $[111]$ cubic direction. At the classical level, energetics further require a vanishing net magnetic moment on each elementary tetrahedron of the pyrochlore lattice. Particularly interesting is the fact that among all classically degenerate ground states that satisfy such zero tetrahedral moment configuration, the material orders at a critical temperature $T_c \approx 1.2$ K in a ground state that breaks a *discrete symmetry* within the local $[111]$ xy plane – the so-called ψ_2 basis state of the Γ_5 irreducible representation (see Fig. 1). [6, 8] Since the original determination [6] of the long-range order in $\text{Er}_2\text{Ti}_2\text{O}_7$, two rather puzzling questions had been identified: Firstly, how could the system order into a state that does not minimize the dipolar interactions, the so-called

Palmer-Chalker state [10] which has each spin in its local xy plane? Secondly, what mechanism may lead to the ψ_2 selection, as opposed to the other ψ_3 basis vector of the two-dimensional Γ_5 manifold (see Fig.1), or even an arbitrary superposition of ψ_2 and ψ_3 arising from a spontaneous XY ($U(1)$) global symmetry breaking?

Earlier studies had shown thermal [6, 11, 12] and quantum [12] ObD selecting a ψ_2 state in a simplified pyrochlore antiferromagnetic XY model. More recent work found that anisotropic exchange can efficiently compete with dipolar interactions and lower the energy of Γ_5 below that of the Palmer-Chalker state. [13] Building on these results, Savary *et al.* [5] showed that the classical degeneracies within Γ_5 are in fact immune to anisotropic bilinear spin-spin interactions of arbitrary form and range, leaving quantum ObD (q-ObD) as essentially [14] the only plausible mechanism explaining the ψ_2 low-temperature state in $\text{Er}_2\text{Ti}_2\text{O}_7$. A similar conclusion was reached in Ref. [9]. The possible occurrence of ObD in $\text{Er}_2\text{Ti}_2\text{O}_7$ represents a potentially significant result in the field of highly frustrated magnetism.

While the arguments of Ref. [5] as per the symmetry-protection of degeneracy are compelling, there is still reason to worry whether the ordering mechanism in $\text{Er}_2\text{Ti}_2\text{O}_7$ has indeed been fully unveiled. In particular, one may ask whether the model of Ref. [5] describes accurately the thermodynamic behavior of $\text{Er}_2\text{Ti}_2\text{O}_7$ close to the transition and predict a $T_c \sim 1.2$ K in accord with experiment. For example, since this was not investigated in Ref. [5], a concern one might have is whether the model, for ignoring the long-range part of the dipole-dipole interactions [15] and other perturbations, does display a thermal ObD at T_c in the correct ψ_2 state, rather than ψ_3 , which would then be inconsistent with experiments. [16] Conversely, one may ask whether the experimentally observed ψ_2 state at low T is the true ground state of the material or a metastable relic of the thermal ObD at T_c . [17] Finally, the recent observation that there exists a tendency for rare-earth ions (e.g. $\text{R}=\text{Er}^{3+}$) in $\text{R}_2\text{Ti}_2\text{O}_7$ pyrochlore oxides to occupy the Ti^{4+} site at the 1% level, [18] hence generating effective random magnetic interactions, also raises concerns whether a plausible q-ObD at low temperatures smoothly merges to its thermal variant at T_c .

The concerns above can only be alleviated by directly addressing, as we do in this paper, whether the model of Ref. [5] describes well the thermodynamic behavior of $\text{Er}_2\text{Ti}_2\text{O}_7$ above T_c . To do so, we use high-temperature expansions (HTE) and crystal-field theory to study the magnetic specific heat and susceptibility of the model. We also calculate order-parameter susceptibilities for ψ_2 and ψ_3 , finding that the model displays a continuous phase transition at a $T_c \approx 1.2$ K close to the experimental value. By calculating a non-linear susceptibility, we show that ψ_2 order is indeed selected by thermal ObD. These results imply that the long-range part of the dipolar interactions neglected in Ref. [5] are not important above T_c [15] and that the model of Ref. [5] is quantitatively accurate. We are thus rather confident that ObD, both thermal and quantum, cooperate in $\text{Er}_2\text{Ti}_2\text{O}_7$ to select ψ_2 over the whole temperature range $0 < T \leq T_c$.

Model & method – In a number of pyrochlore oxides [19], the single-ion crystal-field magnetic doublet ground state is separated from the lowest excited crystal-field energy levels by an energy gap Δ that is large compared to the microscopic interactions, \mathcal{H}_{mic} , between the ions. This is the case for $\text{Er}_2\text{Ti}_2\text{O}_7$ for which $\mathcal{H}_{\text{mic}} \sim 1$ K while $\Delta \sim 75$ K. In such a case, one can use an effective spin-1/2 Hamiltonian \mathcal{H} with bilinear anisotropic couplings, J_s , to describe the interactions between ions, and where \mathcal{H} is the projection of \mathcal{H}_{mic} onto the Hilbert space spanned by the single-ion ground doublets. On symmetry grounds, the nearest-neighbor \mathcal{H} can be parametrized by four exchange parameters as follows:

$$\mathcal{H} = \sum_{\langle i,j \rangle} \{ J_{zz} S_i^z S_j^z - J_{\pm} (S_i^+ S_j^- + S_i^- S_j^+) + J_{\pm\pm} [\gamma_{ij} S_i^+ S_j^+ + \gamma_{ij}^* S_i^- S_j^-] + J_{z\pm} [S_i^z (\zeta_{ij} S_j^+ + \zeta_{ij}^* S_j^-) + i \leftrightarrow j] \} \quad (1)$$

Here, $\langle i,j \rangle$ refers to nearest-neighbor sites of the pyrochlore lattice, γ_{ij} is a 4×4 complex unimodular matrix, and $\zeta = -\gamma^*$ [5, 20]. The \hat{z} quantization axis is along the local [111] direction, and \pm refers to the two orthogonal local directions. The J_s were determined from fits to inelastic neutron scattering spectra in the field polarized state. [5, 21] The magnetic properties of the system are described by the Zeeman Hamiltonian, $\mathcal{H}_Z = -g_L \mu_B \sum_i \mathbf{J}_i \cdot \mathbf{B}$ added to \mathcal{H} , where \mathbf{J} is the $J = 15/2$ angular momentum operator of Er^{3+} , \mathbf{B} is the applied magnetic field, μ_B is the Bohr magneton and $g_L = 6/5$ is the Er^{3+} Landé factor. [22] In this paper we investigate the thermodynamic properties of \mathcal{H} above and near T_c using HTE. [23]

We have computed series for the following quantities: (1) log of the partition function, $\ln Z$, from which heat capacity and entropy are readily calculated; (2) uniform susceptibility as a linear response to a static applied external magnetic field; (3) linear order parameter susceptibilities, χ_{xx} and χ_{yy} , corresponding to ψ_2 and ψ_3 order, respectively; and (4) non-linear (4th and 6th order) order parameter cumulants associated with ψ_2 and ψ_3 long-range order. We discuss below the reason for calculating non-linear susceptibilities from these cumulants. [17]

Demonstrating the validity of \mathcal{H} – We first show evidence that the Hamiltonian (1) is consistent with a phase transition to long-range order in the xy components of the spins at a critical temperature $T_c \sim 1.2$ K. To do so, we calculate high temperature series expansions for the xy order-parameter susceptibilities. We apply a field along the local x (y)-axis at all sites, and calculate the linear response order-parameter susceptibility, χ_{xx} (χ_{yy}). Detailed expressions can be found in the supplementary material [17]. As discussed in Refs. [5, 9], there is an emergent continuous symmetry in the model (1), which is only weakly lifted by higher order effects beyond classical ground state energetics. In the notation of Ref. [5], this classical degeneracy can be parameterized by a continuous angle α . Then, χ_{xx} is the susceptibility for $\alpha = 0$ order (i.e. ψ_2 order) while χ_{yy} is the

susceptibility for $\alpha = \pi/6$ order (i.e. ψ_3 order). We find that the two linear susceptibilities have *identical* high temperature series expansions to the order calculated (8th order in β). We believe that this result is true to all orders and the selection of order within the Γ_5 manifold must therefore only be manifest in non-linear order parameter susceptibilities. We return to this matter later. We study the singularities of the order-parameter susceptibility using d-log Padé approximants. [23] Various estimated T_c and critical exponents γ from near diagonal d-log Padé values, expressed in the form of $(L, M; T_c, \gamma)$ sets, are $(3, 4; 1.26, 1.21)$, $(4, 3; 1.25, 1.71)$, $(3, 3; 1.33, 1.19)$ and $(2, 4; 1.28, 1.14)$ where T_c is in Kelvin. Although the convergence is not excellent for this short series, we nevertheless conclude that the transition temperature is $T_c = 1.2 \pm 0.1$ K. Given the large uncertainty in T_c we cannot make a reliable estimate for γ , but its $\gamma = 1.3 \pm 0.4$ value is consistent with γ values known for 3-dimensional spin models. A plot of the order parameter susceptibility ($\chi_{xx} = \chi_{yy}$) versus temperature is shown in the inset of Fig. 2.

Next, we turn to a calculation of the specific heat, $C(T)$, and its comparison with experiments. We have calculated specific heat using both Numerical Linked Cluster (NLC) method [24–26] and HTE. The two methods agree well at $T > 2$ K. At lower temperatures, the HTE method is better as it allows us to analyze the behavior near the phase transition, where the correlation length diverges. Since we expect the system to display a three-dimensional XY universality class, for which the specific heat exponent α is known to be very close to zero, we bias the analysis of the specific heat series to have a log singularity at $T_c = 1.2$ K. The biased analysis shows good convergence with several approximants found to be very close to each other. A representative plot is shown together with experimental data in Fig. 2, where an excellent agreement with experimental data is seen. The phonon contributions are clearly seen to be negligible below 2 K. The magnetic entropy above T_c can be found in the supplementary material. [17] Its value at T_c is reduced from the infinite temperature value by less than 50 percent, not atypical of 3-dimensional critical points.

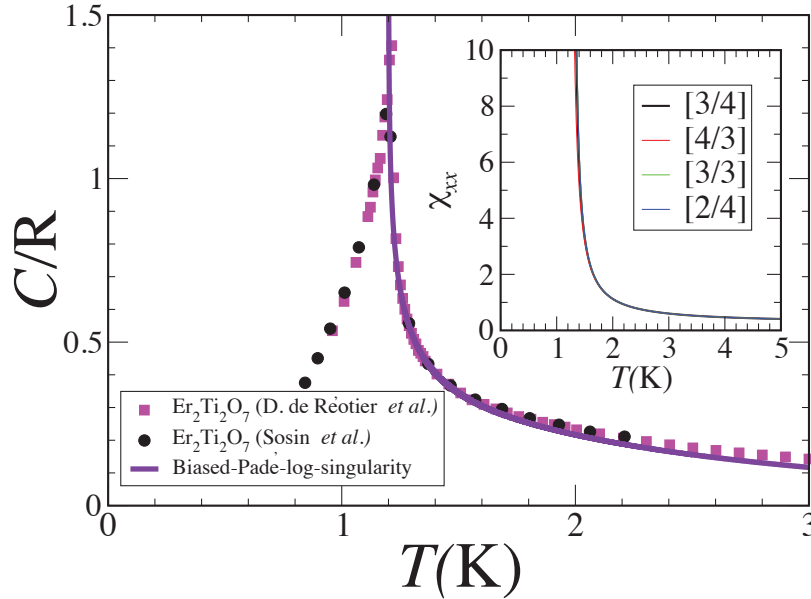


FIG. 2: Thermodynamic behavior of model (1) compared to experimental data. The main panel shows specific heat data for $\text{Er}_2\text{Ti}_2\text{O}_7$ compared with Padé approximants for the high temperature series expansions biased to have a logarithmic singularity at T_c . The experimental data are from Dalmas de Réotier *et al.* [27] and Sosin *et al.* [28]. The inset shows plots of the order parameter susceptibility ($\chi_{xx} = \chi_{yy}$) calculated from high temperature expansions for various dlog Padé approximants (see text).

We now turn to the uniform magnetic susceptibility, which has been measured up to 300 K. As shown in Fig. 4, this data shows a crossover from a high temperature Curie constant of $11.5 \text{ emu/mol} \cdot \text{K}$ to a low temperature Curie constant of $2.48 \text{ emu/mol} \cdot \text{K}$, reflecting the evolution of the material from a $J = 15/2$ system to an effective spin-1/2 system. To understand this susceptibility data, we use HTE to calculate the susceptibility for the effective spin-1/2 model with g_\perp and g_{zz} g -tensor components [22] from Ref. [5], but also the full single-ion susceptibility, $\chi_{\text{s.i.}}$, obtained by including all the crystal-field states of the crystal-field Hamiltonian of $\text{Er}_2\text{Ti}_2\text{O}_7$. [29] The latter is obtained by treating the infinitesimal magnetic field \mathbf{B} that couples to the non-interacting rare-earth ion with second order (degenerate) perturbation theory. [30] The single-ion susceptibility ($\chi_{\text{s.i.}}$) then takes

the form:

$$\chi_{\text{s.i.}} = g_L^2 \mu_0 \mu_B^2 N_A \frac{\sum_n [\beta(E_n^{(1)})^2 - 2E_n^{(2)}] e^{-\beta E_n^{(0)}}}{\sum_n e^{-\beta E_n^{(0)}}}. \quad (2)$$

Here $E_n^{(0)}$ is the energy of the n -th state of H_{CF} while $E_n^{(1)}$ and $E_n^{(2)}$ are the first and second order perturbation theory coefficient of the energy of the n^{th} state, respectively. [30, 31] N_A is the Avogadro number and μ_0 the vacuum permeability.

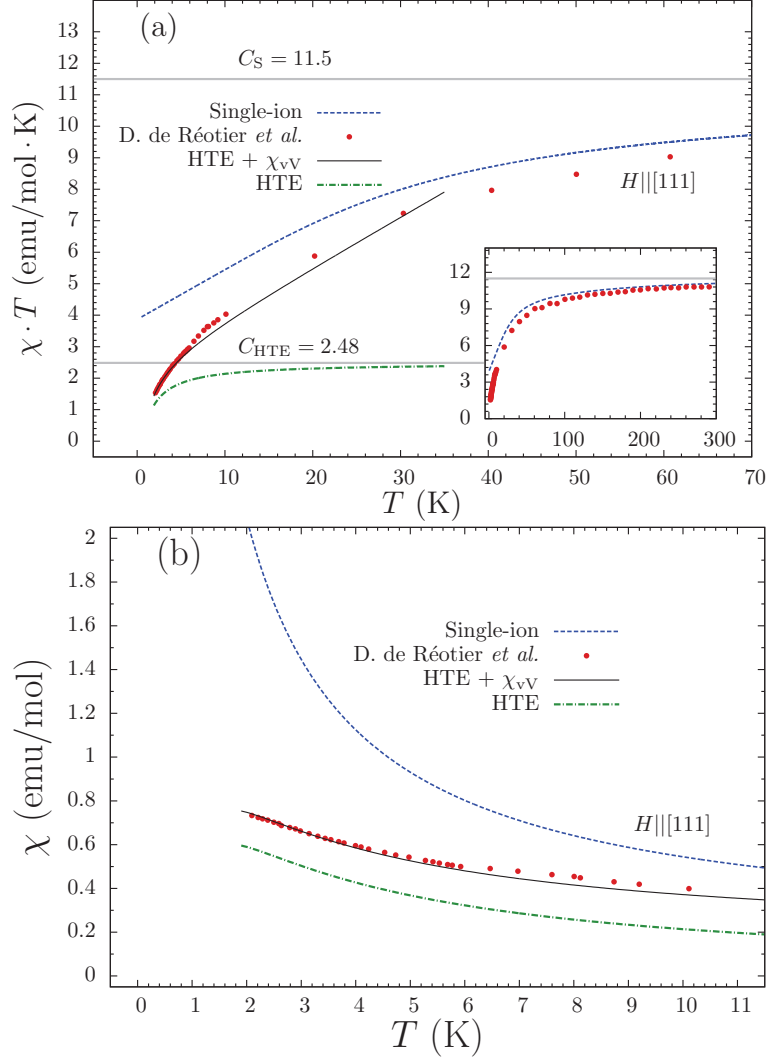


FIG. 3: (a) [111] zero field uniform susceptibility, χ , times temperature, T , versus T . The dashed blue line corresponds to the single-ion calculations which agree with the experimental data of Dalmas de Réotier *et al.* [27] at high temperatures (see inset). The top horizontal gray line corresponds to the calculated Curie constant, $C_S = 11.5$ emu/mol · K. The dashed green line corresponds to the 6th order HTE susceptibility using the Hamiltonian (1). Its corresponding Curie constant is also shown as a gray line with value of $C_{\text{HTE}} = 2.48$ emu/mol · K. The van Vleck susceptibility, $\chi_{\text{vV}} = 0.158$ emu/mol, originating from the admixing of the ground doublet with excited crystal-field states and obtained from the single-ion calculation, is added to the HTE susceptibility to yield the black curve. (b) The low temperature ($T \lesssim 10$ K) susceptibility is reasonably well accounted by the HTE susceptibility corrected with the van Vleck susceptibility.

The inset of Fig. 3(a) shows a comparison of the measured susceptibility with $\chi_{\text{s.i.}}$. The agreement at high temperatures is apparent. The increasing disagreement between the experimental χ and the calculated $\chi_{\text{s.i.}}$ as T is reduced is caused by the progressive development of *antiferromagnetic* correlations which decrease the uniform susceptibility. The main plot shows that below about 70 K, $\chi_{\text{s.i.}}$ deviates significantly from the measured values. Also shown in Fig. 3(a) and Fig. 3(b) are comparisons with the susceptibility calculated by HTE for the projected spin-1/2 model (1) taken alone. The latter saturates to a Curie law C_{HTE}/T form with $C_{\text{HTE}} = 2.48$ emu/mol · K at high temperatures. The HTE expansion considers AF correlations within

the low-energy Hilbert space spanned by the single-ion crystal-field doublets of interacting Er^{3+} ions. These HTE calculations ignore the residual $T \lesssim 10$ K *temperature-independent* contribution coming from the excited crystal-field states, which is the so-called van Vleck susceptibility, χ_{vV} . [30, 31] To compare experimental data with model calculations, we thus need to add χ_{vV} to the HTE calculation results. As seen in Fig. 4(b), one obtains a very good agreement with the experimental data once χ_{vV} is added.

Thermal ObD into ψ_2 – Having demonstrated that the model in Eq. (1) describes the thermodynamic properties of the material above T_c accurately, we now turn to the central question of thermal ObD at T_c . We have already shown that the linear order-parameter susceptibility fails to distinguish between ψ_2 and ψ_3 order upon approaching T_c from the paramagnetic phase. To further address this issue, we need to calculate non-linear order-parameter susceptibilities constructed from equal-time 4th and 6th power cumulants of the ψ_2 and ψ_3 order parameters in HTE. We find that the 4th power cumulant is also identical for the two cases. However, the 6th power of the order parameter does distinguish between ψ_2 and ψ_3 order (see Table VI in the supplementary materials [17]). The necessity to compute a non-linear susceptibility that is 6th order in the order-parameter to reveal the selection of ψ_2 vs ψ_3 can be understood on the basis that a 6th order effective “potential”, $V(\alpha)$, ($V(\alpha) \sim g_6 \cos(6\alpha)$) where $g_6 < 0$ and $g_6 > 0$ selects ψ_2 and ψ_3 , respectively) in the Ginzburg-Landau free-energy is dynamically generated by thermal and quantum fluctuations. [5, 13] Starting at order β^4 , the 6th non-linear order susceptibility for ψ_2 order (or $\alpha = 0$) gets larger than for ψ_3 for every β^n ($n \geq 4$) order considered. [17] This 6th order susceptibility exposes a thermal order by disorder that coincides with the pattern of order selected at $T = 0$ in the works of Savary *et al.*[5] and Zhitomirsky *et al.*[9] (whose model is slightly different from the one we study).

Conclusion – We have shown that the nearest-neighbor spin Hamiltonian (1), with exchange parameters determined from inelastic neutron scattering, [5] describes the thermodynamic properties of $\text{Er}_2\text{Ti}_2\text{O}_7$ at $T > T_c$, including the continuous phase transition at T_c rather adequately. This was demonstrated through detailed comparison of calculated and experimental specific heat ($C(T)$) and uniform susceptibility ($\chi(T)$) data. While the nearest-neighbor part of the dipolar interactions is implicitly incorporated in the model, [15] it lacks such terms beyond nearest neighbors. In spite of that, the thermodynamic properties are described quite well. Similar conclusions were recently reached about a nearest-neighbor model determined by inelastic neutron scattering for the material $\text{Yb}_2\text{Ti}_2\text{O}_7$. [20, 25, 26]

We have also shown that in the paramagnetic phase, the linear order-parameter susceptibility does not reveal the lifting of the Γ_5 manifold degeneracy. The selection of ψ_2 order is only evinced through a non-linear susceptibility that is 6th order in the order-parameter. The thermal order-by-disorder identified in this paper was found to occur in the ψ_2 state, in agreement with experiments [6–8] and with the quantum order-by-disorder calculations of Refs. [5, 9]. We thus conclude that the material $\text{Er}_2\text{Ti}_2\text{O}_7$ presents a unique and convincing case of *co-operating* quantum and thermal order-by-disorder in a frustrated quantum antiferromagnet.

We thank Behnam Javanparast, Anson Wong and Zhihao Hao for useful discussions. This work is supported in part by NSF grant number DMR-1004231 (RRPS), the NSERC of Canada, the Canada Research Chair program (M.G., Tier 1) and by the Perimeter Institute for Theoretical Physics.

-
- [1] J. Villain, R. Bidaux, J.-P. Carton, and R. Conte, J. Phys. France **41**, 1263 (1980).
 - [2] E. F. Shender, Sov. Phys. JETP **56**, 178 (1982).
 - [3] R. Barnett, S. Powell, T. Grass, M. Lewenstein, and S. Das Sarma Phys. Rev. A **85**, 023615 (2012), and references therein.
 - [4] T. Yildirim, Turkish Journal of Physics **23**, 47 (1999).
 - [5] L. Savary, K. A. Ross, B. D. Gaulin, J. P. C. Ruff, and Leon Balents, Phys. Rev. Lett. **109**, 167201 (2012).
 - [6] J. D. M. Champion, M. J. Harris, P. C. W. Holdsworth, A. S. Wills, G. Balakrishnan, S. T. Bramwell, C. Čížmár, T. Fennell, J. S. Gardner, J. Lago, D. F. McMorrow, M. Orendáč, A. Orendáčová D. McK. Paul, R. I. Smith, M. T. F. Telling, and A. Wildes Phys. Rev. B **68**, 020401 (2004).
 - [7] J. P. C. Ruff, J. P. Clancy, A. Bourque, M. A. White, M. Ramazanoglu, J. S. Gardner, Y. Qiu, J. R. D. Copley, M. B. Johnson, H. A. Dabkowska, and B. D. Gaulin Phys. Rev. Lett. **101**, 147205 (2008).
 - [8] A. Poole, A. S. Wills, and E. Lelièvre-Berna, Journal of Physics: Condensed Matter **19**, 452201 (2007).
 - [9] M. E. Zhitomirsky, M. V. Gvozdkova, P. C. W. Holdsworth, R. Moessner, Phys. Rev. Lett. **109**, 077204 (2012).
 - [10] S. E. Palmer and J. T. Chalker, Phys. Rev. B **62** 488 (2000).
 - [11] J. D. M. Champion and P. C. W. Holdsworth, Journal of Physics: Condensed Matter **16**, S665 (2004).
 - [12] P. Stasiak, P. A. McClarty, and M. J. P. Gingras, arXiv:1108.6053 (2011).
 - [13] P. A. McClarty, S. H. Curnoe, and M. J. P. Gingras, Journal of Physics: Conference Series **145**, 012032 (2009).
 - [14] We omit here the tenuous energetic mechanism selection of ψ_2 discussed in Ref. [13] and which involves a high-order van Vleck -like susceptibility.
 - [15] The magnetostatic dipole-dipole interactions, written as $\mathcal{H}_D = \sum_{i>j} (\mu_0\mu_B^2/4\pi) g_{\alpha\gamma} g_{\beta\delta} S_i^\gamma S_j^\delta (r_{ij}^{-3} \delta_{\alpha\beta} - 3r_{ij}^{-5} r_{ij}^\alpha r_{ij}^\beta)$, have their nearest-neighbor part implicitly incorporated in the J_s parameters of \mathcal{H} in Eq. (1) and their contribution beyond nearest neighbors neglected.

- [16] It is possible in principle to have a different low-temperature state stabilized by q-ObD than the state found at $T \lesssim T_c$ that is selected by thermal ObD. For example, a double-transition sequence paramagnetic $\rightarrow \psi_2 \rightarrow \psi_3$ is observed in a classical Heisenberg pyrochlore antiferromagnet model with “indirect” Dzyaloshinskii-Moriya interactions. G.-W. Chern, arXiv:1008.3038 (2010).
- [17] See Supplementary Material.
- [18] K. A. Ross, Th. Proffen, H. A. Dabkowska, J. A. Quilliam, L. R. Yaraskavitch, J. B. Kycia, and B. D. Gaulin, Phys. Rev. B, **86**, 174424 (2012).
- [19] J. S. Gardner, M. J. P. Gingras, and J. E. Greedan, Rev. Mod. Phys. **82**, 53 (2010).
- [20] K. A. Ross, L. Savary, B. D. Gaulin and L. Balents, Phys. Rev. X **1**, 021002 (2011).
- [21] The numerical values of those J_s couplings are, (in Kelvin): $J_{\pm} = 0.754 \pm 0.087$, $J_{\pm\pm} = 0.487 \pm 0.058$, $J_{zz} = -0.290 \pm 0.21$ and $J_{z\pm} = -0.102 \pm 0.18$. The two largest couplings are of the XY type and the physics is thus very different from spin ice (see for example Ref.[20]).
- [22] The components of \mathbf{J} entering in \mathcal{H}_Z projected in the ground doublet are expressed as $J_i^\alpha = g_{\alpha\beta} S_i^\beta$ where α, β are cartesian components and sum over repeated indices is implied. $g_{\alpha\beta}$ are the elements of the g -tensor with principal axes along the local x, y and z directions with eigenvalues $g_{xx} = g_{yy} \equiv g_{\perp} = 5.97$ and $g_{zz} = 2.45$ from Ref. [5].
- [23] J. Oitmaa, C. Hamer and W. Zheng, *Series Expansion Methods for strongly interacting lattice models*, Cambridge University Press (2006).
- [24] M. Rigol, T. Bryant and R. R. P. Singh, Phys. Rev. Lett. **97**, 187202 (2006).
- [25] R. Applegate, N. R. Hayre, R. R. P. Singh, T. Lin, A. G. R. Day, and M. J. P. Gingras, Phys. Rev. Lett. **109**, 097205 (2012).
- [26] N. R. Hayre, K. A. Ross, R. Applegate, T. Lin, R. R. P. Singh B. D. Gaulin, and M. J. P. Gingras, arXiv:1211.5934 (2012).
- [27] P. Dalmas de Réotier, A. Yaouanc, Y. Chapuis, S. H. Curnoe, B. Grenier, E. Ressouche, C. Marin, J. Lago, C. Baines, and S. R. Giblin, Phys. Rev. B **86**, 104424 (2012).
- [28] S. S. Sosin, L. A. Prozorova, M. R. Lees, G. Balakrishnan, and O. A. Petrenko, Phys. Rev. B **82**, 094428 (2010).
- [29] A. Bertin, Y. Chapuis, P. Dalmas de Réotier, and A. Yaouanc. Journal of Physics: Condensed Matter **24**, 256003 (2012).
- [30] R.M. White, *Quantum Theory of Magnetism: Magnetic Properties of Materials*, Springer Series in Solid-State Sciences. Springer (2010).
- [31] J. Jensen and A. R. Mackintosh, *Rare Earth Magnetism*, (Clarendon Press, Oxford, 1991).
- [32] The addition of pseudo-dipolar or indirect Dzyaloshinskii-Moriya interactions, such as those considered in Ref. [13], renormalize the critical value of the magnetostatic dipolar interaction at which thermal ObD to ψ_2 occurs in Ref. [12] despite the ground state being Palmer-Chalker. [10]
- [33] A Monte Carlo study of a classical Heisenberg antiferromagnet model that interpolates between a face-centered cubic lattice and a pyrochlore found that the thermal order-by-disorder always overcomes the energetic selection down to the lowest temperature. [C. Pinettes, B. Canals, and C. Lacroix, Phys. Rev. B **66**, 024422 (2002).]
- [34] We thank B. Gaulin, K. Ross and J. Ruff and K. Rule for correspondence on this matter.

SUPPLEMENTAL MATERIAL

This section provides supplemental material to the main part of our paper. Firstly, we discuss the hypothetical situation when the thermal order-by-disorder can lead to a different long-range ordered state than the quantum order-by-disorder. Secondly, we provide some details regarding the high-temperature series expansion, in particular in regards to the order parameter linear and non-linear susceptibilities. Then we show the results for the temperature dependence of the magnetic entropy, $S(T)$, corresponding to the magnetic specific heat $C(T) = TdS/dT$ presented in the body of the paper. Finally, we provide tables for the high-temperature series expansion of various quantities of interest and referred to in the main text.

Metastability of States Selected by Thermal Order-by-Disorder

One may ask whether the long-range ordered state that is selected at the critical temperature differs from the zero-temperature ground state selected by quantum fluctuations. In case, thermal and quantum ObD are different, there is a possibility of metastability of the thermal ObD state at low temperatures. Thus, the concern here has to do with the kinetics in the real material rather than thermodynamics. Unlike natural proteins, extensively degenerate systems may lack funneled free-energy landscapes. As a result, configuration-space pathways and dynamical access to states may play a role in the specific long-range ordered phases experimentally realized. Ref. [5] finds a zero-point energy stabilization (δE_0) of ψ_2 compared to ψ_3 of merely $\delta E_0 \sim 0.3 \mu\text{eV}$ (a factor 1/30 of the reported smallest anisotropic exchange. [5]) One may then ask whether the neglected interactions *beyond* nearest neighbors, in particular the dipolar interactions of magnitude $10 \mu\text{eV} \sim 30\delta E_0$, [15] may have instead led to a ψ_3 ground state via quantum ObD. Meanwhile, *thermal* ObD, not considered in Ref. [5], may in fact be responsible for a transition into ψ_2 at T_c , both in the material and in an amended version of the model of Ref. [5] that would incorporate interactions neglected therein. [16] Following such a thermal ObD into ψ_2 in the material, a lower temperature ordering into ψ_3 , or even in the Palmer-Chalker state, may be dynamically inhibited, similar to what is found in Monte Carlo simulations of a pyrochlore XY antiferromagnet with weak dipolar interactions. [12, 32, 33] In such a scenario, the model of Ref. [5] would seemingly predict the correct low-temperature state of $\text{Er}_2\text{Ti}_2\text{O}_7$ – but for the wrong reasons. To rule out the possibility of metastability of ψ_2 at low temperatures, one could cool down to a high-field phase and gradually lower the field at low temperatures to assess whether ψ_2 is still realized. To our knowledge, such an experiment has not been carried out. [34]

Notes on High Temperature Series Expansion for $\text{Er}_2\text{Ti}_2\text{O}_7$

We consider the Hamiltonian

$$\mathcal{H} = \mathcal{H}_e + H_Z + H_x + H_y, \quad (3)$$

Here \mathcal{H}_e is the exchange Hamiltonian defined in terms of local spin variables and exchange constants J_{zz} , $J_{z\pm}$, J_{\pm} and $J_{\pm\pm}$. The next term H_Z is the Zeeman term arising from the applied external field \mathbf{B} which, for a field along $[111]$, can be written in terms of local spin variables as

$$\begin{aligned} \mathcal{H}_Z = & -B [g_{zz}S_0^z - \frac{1}{3}g_{zz}(S_1^z + S_2^z + S_3^z) \\ & - \frac{2\sqrt{2}}{3}g_{xy}S_1^x + \frac{\sqrt{2}}{3}g_{xy}(S_2^x + S_3^x) - \sqrt{\frac{2}{3}}g_{xy}(S_2^y - S_3^y)]. \end{aligned} \quad (4)$$

Here the subscripts 0, 1, 2 and 3 denote different sublattices and one needs to sum over all sites. The last two terms in the Hamiltonian are auxiliary field terms introduced for computational purposes.

$$H_x = -h_x \sum_i S_i^x \quad (5)$$

and

$$H_y = -h_y \sum_i S_i^y. \quad (6)$$

All spins are defined in their local basis.

High temperature series expansions are calculated for the logarithm of the zero-field partition function $\ln(Z_0)$, with Z_0 given by

$$Z_0 = \text{Tr} \exp(-\beta \mathcal{H}_e). \quad (7)$$

From $\ln(Z_0)$ the entropy and specific heat series follow by simple differentiation.

The zero field uniform susceptibility is calculated as the second derivative of the free energy with respect to the applied external magnetic field, B , with $h_x = h_y = 0$.

$$\chi = \frac{-1}{N\beta} \frac{\partial^2}{\partial B^2} \ln(Z(B)) \Big|_{B=0}. \quad (8)$$

In calculating χ from this equation, one obtains only the contribution from the interacting ions assumed to be in their single-ion crystal field ground states and neglecting any contribution from excited crystal field levels. To reach quantitative agreement with experiments, one needs to incorporate the residual low-temperature contribution to the susceptibility coming from the excited crystal field states. This is the so-called van Vleck susceptibility. [30, 31]

To calculate the order-parameter susceptibility for ψ_2 , we set $B = h_y = 0$ and calculate the second derivative of the free energy with respect to h_x .

$$\chi_{xx} = \frac{-1}{N\beta} \frac{\partial^2}{\partial h_x^2} \ln(Z(h_x)) \Big|_{h_x=0} \quad (9)$$

Similarly, for ψ_3 , order we set $B = h_x = 0$ and take second derivative of free energy with respect to h_y

$$\chi_{yy} = \frac{-1}{N\beta} \frac{\partial^2}{\partial h_y^2} \ln(Z(h_y)) \Big|_{h_y=0} \quad (10)$$

Evidently the series for χ_{xx} and χ_{yy} are identical.

Non-linear susceptibilities do not appear to have linked-cluster property. Instead, higher order zero field cumulants were calculated by Linked cluster expansion. These are analogous to equal-time structure factors (rather than zero-frequency susceptibilities). Setting $B = h_x = h_y = 0$, we define for $\alpha = x$ or $\alpha = y$ the order-parameter operator

$$M_\alpha \equiv \sum_i S_i^\alpha. \quad (11)$$

Then, the cumulants, $C_{n,\alpha}$, are:

$$C_{2,\alpha} \equiv \langle M_\alpha^2 \rangle, \quad (12)$$

$$C_{4,\alpha} \equiv \langle M_\alpha^4 \rangle - 3\langle M_\alpha^2 \rangle^2, \quad (13)$$

and

$$C_{6,\alpha} \equiv \langle M_\alpha^6 \rangle - 15\langle M_\alpha^4 \rangle \langle M_\alpha^2 \rangle + 30\langle M_\alpha^2 \rangle^3. \quad (14)$$

Here, one should note that the bare moments $\langle M_\alpha^4 \rangle$ and $\langle M_\alpha^6 \rangle$ do not satisfy linked cluster property but the $C_{n,\alpha}$ cumulants do. Since $\langle M_\alpha^2 \rangle$ and $\langle M_\alpha^4 \rangle$ are identical term by term, the difference $\langle M_x^6 \rangle - \langle M_y^6 \rangle$ is equal to the difference in the cumulants, $\langle C_{6,x} \rangle - \langle C_{6,y} \rangle$.

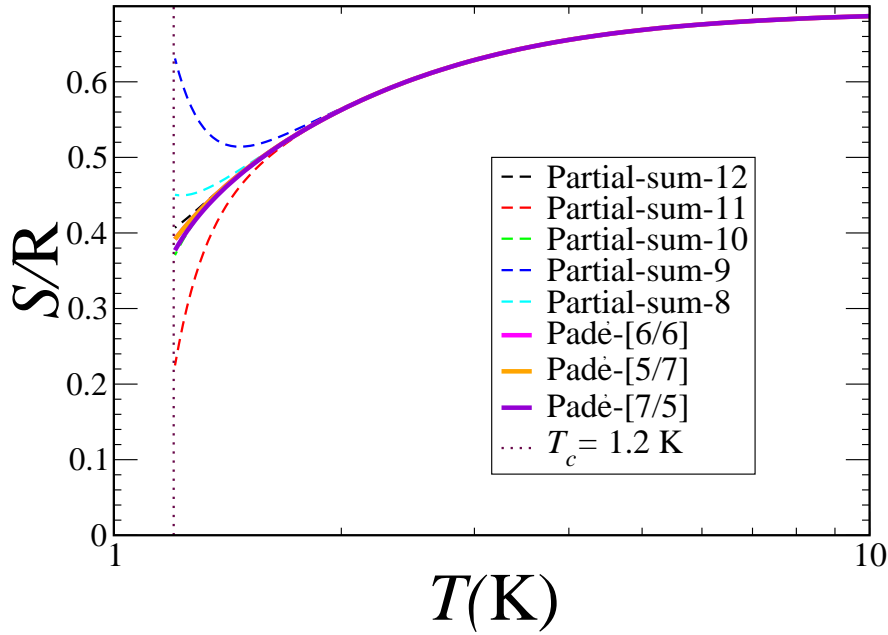


FIG. 4: A plot of the entropy function for the model. The dotted line shows the estimated critical point. The calculations presented here are only informative above T_c .

TEMPERATURE DEPENDENCE OF THE MAGNETIC ENTROPY, $S(T)$

The magnetic entropy function, $S(T)$, is shown in Fig. 4. We show the partial sums of the series from order 8 to order 12 as well as a few Padé approximants. At the critical temperature the entropy per mole in units of the perfect gas constant R is around 0.4. In other words, it is reduced from the infinite temperature value, $S_\infty = R \ln(2)$, by less than fifty percent. This is not unusual compared to typical three-dimensional phase transitions to long-range order. This indicates that the system is not highly frustrated with the development of a strongly correlated regime above T_c . A similar conclusion was reached in Ref. [5] on the basis of a comparison between the mean-field critical temperature of the model, $T_c^{\text{mf}} \sim 2.3$ K, and the experimentally observed $T_c = 1.2$ K.

High-Temperature Series for Various Quantities

In this section, we provide the reader with tables of coefficients for the high-temperature series of quantities of interest. Unless stated otherwise, the high-temperature series of a quantity, $Q(T)$, as a function of inverse temperature $\beta \equiv 1/T$ (with temperature T in Kelvin), is expressed in the form

$$Q(T) = \sum_{n=0}^{n_{\text{max}}} a_n \beta^n. \quad (15)$$

TABLE I: $\ln(Z)$ (per spin) series with only the two largest J_s (in Kelvin); $J_{\pm} = 0.754$, $J_{\pm\pm} = 0.487$, $J_{zz} = 0$ and $J_{z\pm} = 0$. The label $E \pm m$ means $10^{\pm m}$.

Order n	expansion coefficient a_n
0	+0.693147181 $E +00$
1	+0.000000000 $E +00$
2	+0.604263750 $E +00$
3	+0.802114625 $E -01$
4	-0.218372147 $E +00$
5	-0.863347964 $E -01$
6	+0.158902388 $E +00$
7	+0.120287973 $E +00$
8	-0.958592054 $E -01$
9	-0.118324998 $E +00$
10	+0.361281401 $E -01$
11	+0.728830750 $E -01$
12	+0.335017563 $E -01$

TABLE II: $\ln(Z)$ (per spin) series with all four J_s (in Kelvin); $J_{\pm} = 0.754$, $J_{\pm\pm} = 0.487$, $J_{zz} = -0.290$ and $J_{z\pm} = -0.102$. The label $E \pm m$ means $10^{\pm m}$.

Order n	expansion coefficient a_n
0	+0.693147181 $E +00$
1	+0.000000000 $E +00$
2	+0.619951125 $E +00$
3	+0.604908776 $E -01$
4	-0.257221456 $E +00$
5	-0.662731421 $E -01$
6	+0.223356105 $E +00$
7	+0.103109973 $E +00$
8	-0.200436766 $E +00$
9	-0.120572677 $E +00$
10	+0.186373242 $E +00$
11	+0.113320221 $E +00$
12	-0.155050053 $E +00$

TABLE III: Order parameter susceptibility $\chi_{xx} = \chi_{yy}$ per spin with all four J_s (in Kelvin); $J_{\pm} = 0.754$, $J_{\pm\pm} = 0.487$, $J_{zz} = -0.290$ and $J_{z\pm} = -0.102$. The label $E \pm m$ means $10^{\pm m}$.

Order n	expansion coefficient a_n
0	+0.250000000 $E +00$
1	+0.565500000 $E +00$
2	+0.856772872 $E +00$
3	+0.105521359 $E +01$
4	+0.130532942 $E +01$
5	+0.181908741 $E +01$
6	+0.253686031 $E +01$
7	+0.320904312 $E +01$
8	+0.386983904 $E +01$

TABLE IV: Second order order-parameter $C_{2,x}$ cumulant per spin with all four J_s (in Kelvin); $J_{\pm} = 0.754$, $J_{\pm\pm} = 0.487$, $J_{zz} = -0.290$ and $J_{z\pm} = -0.102$. Each coefficient is the same for the second order $C_{2,y}$ cumulant to the last digit shown. The label $E \pm m$ means $10^{\pm m}$.

Order n	expansion coefficient a_n
0	+0.250000000000 $E +00$
1	+0.565500000000 $E +00$
2	+0.936030375000 $E +00$
3	+0.107532105831 $E +01$
4	+0.123006642254 $E +01$
5	+0.179517883700 $E +01$
6	+0.263550433751 $E +01$
7	+0.325196289151 $E +01$
8	+0.374996212319 $E +01$

TABLE V: Fourth order order-parameter $C_{4,x}$ cumulant per spin with all four J_s (in Kelvin); $J_{\pm} = 0.754$, $J_{\pm\pm} = 0.487$, $J_{zz} = -0.290$ and $J_{z\pm} = -0.102$. Each coefficient is the same for fourth order $C_{4,y}$ cumulant to the last digit shown. The label $E \pm m$ means $10^{\pm m}$.

Order n	expansion coefficient a_n
0	-0.125000000000 $E +00$
1	-0.113100000000 $E +01$
2	-0.532304971875 $E +01$
3	-0.172896459338 $E +02$
4	-0.437448147843 $E +02$
5	-0.961820514195 $E +02$
6	-0.196495861437 $E +03$
7	-0.381391503061 $E +03$
8	-0.704597614446 $E +03$

TABLE VI: Sixth order order-parameter $C_{6,x}$ cumulant and $C_{6,y}$ cumulant per spin with all four J_s (in Kelvin); $J_{\pm} = 0.754$, $J_{\pm\pm} = 0.487$, $J_{zz} = -0.290$ and $J_{z\pm} = -0.102$. The label $E \pm m$ means $10^{\pm m}$. The last column shows the difference between the two cumulants. Note the increasing difference with increasing β^n order.

Order n	expansion coefficient a_n ($C_{6,x}$ -cumulant)	expansion coefficient a_n ($C_{6,y}$ -cumulant)	difference
0	+0.250000000000 $E +00$	+0.250000000000 $E +00$	
1	+0.480675000000 $E +01$	+0.480675000000 $E +01$	
2	+0.424661478750 $E +02$	+0.424661478750 $E +02$	
3	+0.243939243681 $E +03$	+0.243939243680 $E +03$	
4	+0.104714406827 $E +04$	+0.104714276704 $E +04$	+0.00130123
5	+0.366000012391 $E +04$	+0.365997458485 $E +04$	+0.02553906
6	+0.110533363334 $E +05$	+0.110532277550 $E +05$	+0.1085784
7	+0.300260377288 $E +05$	+0.300256729522 $E +05$	+0.3647766
8	+0.752398706312 $E +05$	+0.752389652239 $E +05$	+0.9054073

TABLE VII: Uniform susceptibility series per spin with all four J_s (in Kelvin); $J_{\pm} = 0.754$, $J_{\pm\pm} = 0.487$, $J_{zz} = -0.290$ and $J_{z\pm} = -0.102$. The g -tensor values are $g_{\perp} = 6.05$ and $g_{zz} = 2.5$. The infinitesimal applied field is along the $[111]$ cubic direction. The label $E_{\pm m}$ means $10^{\pm m}$. To convert into a susceptibility in $\text{emu/mol} \cdot \text{K}$ units, the given values have to be multiplied by $N_A \mu_B^2 / k_B \approx 0.375$ where N_A , μ_B and k_B are the Avogadro number, Bohr magneton and Boltzmann constant, respectively, all expressed in CGS units.

Order n	expansion coefficient a_n
0	+0.662125000 $E + 01$
1	-0.988978150 $E + 01$
2	+0.683472045 $E + 01$
3	-0.163940184 $E + 01$
4	+0.131075702 $E + 01$
5	-0.379184574 $E + 01$
6	+0.103613852 $E + 01$